Infectious Disease Modelling 9 (2024) 84–102

Contents lists available at ScienceDirect

Infectious Disease Modelling

journal homepage: www.keaipublishing.com/idm

SEIRS model for malaria transmission dynamics incorporating seasonality and awareness campaign

Francis Oketch Ochieng

Department of Pure and Applied Mathematics, Jomo Kenyatta University of Agriculture and Technology, Nairobi, 62000-00200, Kenya

ARTICLE INFO

Article history:
Received 16 September 2023
Received in revised form 5 November 2023
Accepted 30 November 2023
Available online 9 December 2023
Handling Editor: Dr Daihai He

Keywords:
SEIRS model
Malaria transmission dynamics
Model fitting
Basic reproduction number
Stability analysis
Seasonality
Awareness campaign
Runge–Kutta method

ABSTRACT

Malaria, a devastating disease caused by the Plasmodium parasite and transmitted through the bites of female Anopheles mosquitoes, remains a significant public health concern, claiming over 600,000 lives annually, predominantly among children. Novel tools, including the application of Wolbachia, are being developed to combat malaria-transmitting mosquitoes. This study presents a modified susceptible-exposed-infectious-recovered-susceptible (SEIRS) compartmental mathematical model to evaluate the impact of awareness-based control measures on malaria transmission dynamics, incorporating mosquito interactions and seasonality. Employing the next-generation matrix approach, we calculated a basic reproduction number (R_0) of 2.4537, indicating that without robust control measures, the disease will persist in the human population. The model equations were solved numerically using fourth and fifth-order Runge-Kutta methods. The model was fitted to malaria incidence data from Kenya spanning 2000 to 2021 using least squares curve fitting. The fitting algorithm yielded a mean absolute error (MAE) of 2.6463 when comparing the actual data points to the simulated values of infectious human population (I_h). This finding indicates that the proposed mathematical model closely aligns with the recorded malaria incidence data. The optimal values of the model parameters were estimated from the fitting algorithm, and future malaria dynamics were projected for the next decade. The research findings suggest that social media-based awareness campaigns, coupled with specific optimization control measures and effective management methods, offer the most cost-effective approach to managing malaria.

1. Introduction

Malaria, a prevalent infectious disease primarily transmitted through the bite of infected female Anopheles mosquitoes, remains a significant global health challenge (Traor et al., 2017). The transmission cycle commences when an infected individual is bitten by an Anopheles mosquito, leading to the ingestion of malaria parasites known as gametocytes (Collins & Duffy, 2022). These parasites undergo a series of transformations within the mosquito, eventually maturing into infectious sporozoites that reside in the mosquito's salivary glands (Matuschewski, 2006). During subsequent feedings, the infected

E-mail address: francokech@gmail.com.
Peer review under responsibility of KeAi Communications Co., Ltd.

https://doi.org/10.1016/j.idm.2023.11.010

mosquito injects these sporozoites into the bloodstream of a susceptible individual, initiating a new cycle of malaria transmission (Collins & Duffy, 2022).

The likelihood of malaria transmission is influenced by various factors, including the specific mosquito species involved, the prevalence of malaria parasites within the local population, and environmental conditions such as temperature and humidity (Stresman, 2010). Notably, different Plasmodium parasite species exist, with P. falciparum and P. vivax being the primary culprits behind human malaria infections (Bakary, Boureima, & Sado, 2018; Ndamuzi & Gahungu, 2021).

In 2020, the World Health Organization (WHO) reported an estimated 241 million malaria cases globally, accompanied by approximately 627,000 malaria-related deaths (World Health Organization et al., 2020). Africa bore the brunt of this burden, accounting for 95% of malaria cases and 96% of malaria-related fatalities worldwide (World Health Organization et al., 2020). Alarmingly, within this region, children under the age of 5 accounted for a staggering 80% of overall malaria-related deaths (World Health Organization et al., 2020).

Effective malaria prevention strategies encompass a range of interventions, including the use of insecticide-treated bed nets (ITNs), indoor residual spraying (IRS), antimalarial prophylaxis, and mosquito breeding site control (Prempeh, 2020). These measures aim to reduce mosquito-human contact and impede the spread of malaria.

Mathematical modeling has emerged as a valuable tool for comprehending the intricate dynamics of malaria transmission and guiding control strategies (Mandal, Sarkar, & Sinha, 2011). Epidemiological models, such as the Susceptible-Exposed-Infectious-Removed (SEIR) model, have proven instrumental in capturing the temporal patterns of malaria transmission (Ma, Li, & Warner, 2019). By stratifying populations into compartments based on their infection status, these models enable the estimation of crucial epidemiological parameters, such as the basic reproduction number (R_0).

Mosquito behavior plays a pivotal role in shaping malaria transmission dynamics. Recent modeling studies have incorporated mosquito behavior into mathematical models to evaluate the effectiveness of vector control measures (Chitnis et al., 2010). For instance, Griffin et al.'s model (Griffin et al., 2010) integrates mosquito feeding and resting behavior to assess the impact of ITNs on mosquito populations.

Seasonal variations in climate and mosquito abundance significantly influence malaria transmission patterns (Ezihe et al., 2017). Several recent studies have focused on incorporating seasonality into mathematical models (Ren et al., 2016). These models aid in identifying periods of high transmission risk, enabling more targeted intervention strategies.

The emergence of antimalarial drug resistance poses a substantial threat to malaria control efforts (Ippolito et al., 2021). Mathematical models have been employed to assess the spread of drug-resistant parasites within populations (Mueller et al., 2022). These models inform the design of optimal drug deployment strategies.

Awareness campaigns and their impact on human behavior have also garnered attention in recent modeling endeavors (Basir & Abraha, 2023). These models consider the influence of awareness on the adoption of preventive measures, such as bed nets and insecticides. Social media-based awareness campaigns have been shown to be an effective and cost-effective way to raise awareness about malaria prevention and control. A study by the World Health Organization (WHO) found that social media campaigns can increase knowledge of malaria prevention and control measures by up to 40% (Yaya et al., 2018). Additionally, social media campaigns can be targeted to specific populations, such as pregnant women and children, who are at high risk of contracting malaria.

A study conducted by the London School of Hygiene and Tropical Medicine demonstrated that a combination of social media-based awareness campaigns and Optimal control methods (OCMs) represents the most cost-effective approach to managing malaria (Gallup & Sachs, 2000). Their findings revealed that this approach could potentially save up to $5 billion annually in malaria control costs. A study by the Centers for Disease Control and Prevention (CDC) indicated that social media-based awareness campaigns can increase insecticide-treated bed nets (ITNs) usage by up to 20% (Centers for Disease Control and, 2023). Additionally, a study by the Malaria Atlas Project revealed that OCMs can reduce the incidence of malaria by up to 80% (Walker et al., 2016). Furthermore, a study by the World Bank indicated that the cost of a social media-based awareness campaign is typically less than $0.10 per person (Corrado et al., 2006). Similarly, a study by the WHO revealed that the cost of OCMs is typically less than $1.00 per person (Gabriel et al., 2016).

The current study distinguishes itself from the research conducted by Al-Basir and Abraha (Basir & Abraha, 2023) in several notable aspects. Firstly, it employs a unique compartmental model structure, deviating from the one used by Al-Basir and Abraha. Secondly, it introduces a dedicated compartment specifically for mosquitoes, enabling the exploration of nonlinear human-environment interactions, an element missing in Al-Basir and Abraha's model. Additionally, this study conducts an extensive set of simulation studies to meticulously examine the model's behavior under various scenarios, whereas Al-Basir and Abraha's study did not include such simulations. Finally, the developed mathematical model is fitted to real data on malaria infections, and its parameters are optimized using a rigorous optimization algorithm, further enhancing its robustness and applicability.

This study's mathematical model, inspired by the compartmental models in (Traor et al., 2017) and (Basir & Abraha, 2023), will inform the feasibility of control through the strategic implementation of novel interventions. By shedding light on the intricate dynamics of malaria transmission, this model can pave the way for effective malaria prevention and control strategies.

2. Mathematical model development

2.1. Compartmental model formulation

To study the dynamics of malaria transmission in Kenya, we developed a mathematical framework that incorporates the interaction between two distinct groups: the human population acting as hosts and the mosquito population serving as vectors, as depicted in Fig. 1. The model is based on the compartmental modeling approach, which partitions the total population into compartments based on their infection status.

The complexity of the compartmental model presented in this study is a deliberate choice that reflects the intricate nature of malaria transmission dynamics. Malaria is a multifaceted disease influenced by numerous factors, including human behavior, mosquito ecology, environmental conditions, and the interplay between these elements. Oversimplifying these interactions can lead to inaccurate representations of the disease and hinder the development of effective control strategies.

2.1.1. Human population

The human population is divided into five compartments.

1. Susceptible unaware human (S_{hu}): These individuals are susceptible to malaria infection but are unaware of the disease or its prevention measures.
2. Susceptible aware human (S_{ha}): These individuals are susceptible to malaria infection but are aware of the disease and are taking some preventive measures, such as using mosquito nets or insecticides.
3. Exposed human (E_h): These individuals have been bitten by an infected mosquito and are in the incubation period of the disease, meaning they are not yet infectious.
4. Infectious human (I_h): These individuals are carrying the malaria parasite and can transmit the disease to others.
5. Recovered human (R_h): These individuals have recovered from malaria and have developed some immunity to the disease, but this immunity may wane over time.

Hence, the total human population is given by the equation

$$N_h(t) = S_{hu}(t) + S_{ha}(t) + E_h(t) + I_h(t) + R_h(t) \tag{1}$$

The dynamics of the human population are governed by the following transition rates.

- β_1: The rate at which susceptible unaware individuals become infected after being bitten by an infected mosquito.
- β_2: The rate at which susceptible aware individuals become infected after being bitten by an infected mosquito.
- α_1: The rate at which susceptible unaware individuals become susceptible aware due to awareness campaigns.
- α_2: The rate at which susceptible aware individuals revert to susceptible unaware.
- ρ: The rate at which exposed individuals progress to the infectious stage.
- r: The rate at which infectious individuals recover from malaria.
- σ: The rate at which infectious individuals die from malaria.
- φ: The rate at which recovered individuals lose their immunity and become susceptible again.

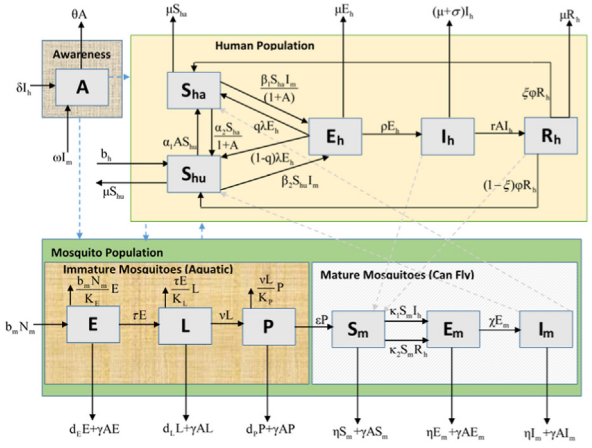

Fig. 1. SEIRS model of malaria transmission. Depicting a human (SEIRS, yellow shade), mosquito (ELPSEI, green shade), and media campaign awareness (A, black shaded) compartmental model.

2.1.2. Mosquito population

The Anopheles mosquito life cycle consists of two main stages: the mature stage, comprising of those mosquitoes that can fly, and the immature stage, also known as the aquatic stage. The immature stage is further divided into three compartments: eggs, larvae, and pupae. The mature mosquito population is subdivided into three compartments: susceptible, exposed, and infectious. Hence, the mosquito population is represented by six compartments.

1. Eggs (E): These are the fertilized eggs laid by female mosquitoes.
2. Larvae (L): These are the immature stages of mosquitoes that develop in water.
3. Pupae (P): These are the final stages of mosquito development before they emerge as adults.
4. Susceptible mosquitoes (S_m): These are adult mosquitoes that have not yet been infected with the malaria parasite.
5. Exposed mosquitoes (E_m): These are adult mosquitoes that have been bitten by an infected human and are in the incubation period of the parasite.
6. Infectious mosquitoes (I_m): These are adult mosquitoes that are carrying the malaria parasite and can transmit the disease to humans.

Hence, the total mature mosquito population is given by the equation

$$N_m(t) = S_m(t) + E_m(t) + I_m(t) \tag{2}$$

The dynamics of the mosquito population are governed by the following transition rates.

- b_m: The per capita oviposition rate of female mosquitoes.
- τ: The rate at which eggs hatch into larvae.
- ν: The rate at which larvae pupate.
- η: The natural mortality rate of adult mosquitoes.
- κ_1: The rate at which susceptible mosquitoes become infected after biting an infectious human.
- κ_2: The rate at which susceptible mosquitoes become infected after biting a recovered human.
- χ: The rate at which exposed mosquitoes become infectious.
- γ: The rate at which mosquito eggs, larvae, and pupae are eliminated through awareness campaigns.

2.1.3. Awareness campaign

Within this framework, the concept of an awareness campaign, represented by $A(t)$, is considered a distinct population. It is hypothesized that media campaigns contribute to increased awareness of self-protection measures and mosquito population reduction strategies. The level of awareness among individuals increases proportionally to the number of infected mosquitoes at a rate denoted as ω, influenced by global information sources like radio and TV. Additionally, awareness also rises in response to local campaigns, with its growth being proportional to the number of infected humans at a rate of δ. Conversely, awareness diminishes at a rate of θ due to memory fading.

2.1.4. Model assumptions

The model is based on the following assumptions.

1. Mosquitoes only bite humans and do not transmit malaria to other mosquitoes.
2. Malaria cannot be directly transmitted through methods such as blood transfusion or from a mother to her baby.
3. Individuals have a natural mortality rate, which is not affected by malaria infection.
4. Individuals who have recovered from malaria have some immunity to the disease, but this immunity may wane over time.
5. Infected individuals can transmit malaria to others for the entire duration of their infection.
6. Mosquitoes have a natural lifespan, which is not affected by malaria infection.
7. Mosquitoes can become infected with the malaria parasite only by biting an infectious human.
8. Infected mosquitoes can transmit malaria to humans only during their infectious period.
9. There are no infected mosquitoes introduced into the community from external sources.

These assumptions are essential for simplifying the complex dynamics of malaria transmission and allowing for a mathematical analysis of the model. They are based on current biological understanding and epidemiological data.

2.1.5. The human-mosquito interaction process

The human population enters the susceptible category at a rate denoted as b_h (encompassing both births and immigration), and experiences a natural mortality rate of μ. Susceptible individuals become aware of the disease and its prevention measures through awareness campaigns, which are disseminated via platforms such as social media, radio, and television. This transition occurs at a rate of α_1. Once aware, individuals are more likely to adopt preventive measures, such as using

mosquito nets and insecticides, which reduce the transmission rate. However, awareness levels can diminish over time, leading to a reversion rate of α_2 from the aware to the unaware state. This reversion rate decreases as awareness levels increase.

The transmission of the malaria parasite from infected female Anopheles mosquitoes to susceptible humans occurs through bites during close contact (Paton et al., 2019). Since female Anopheles mosquitoes have a lifespan of several days, individuals living in or near mosquito breeding sites have a higher likelihood of being bitten. The probability of parasite entry into the human body upon a bite is denoted by β_1 and β_2 for bites from infectious mosquitoes to susceptible humans.

Susceptible humans who are bitten by infected mosquitoes initially progress to the exposed human population, $E_{\mathrm{h}}(t)$, as there is an incubation period before symptoms manifest. After a certain duration, these exposed individuals transition to the infectious population, $I_{\mathrm{h}}(t)$, at a rate denoted by ρ. A majority of those in the infectious group recover at a rate denoted by r and subsequently join the recovered human population, designated as $R_{\mathrm{h}}(t)$, after acquiring immunity. The recovery of infectious individuals is contingent upon the effectiveness of the awareness campaign. Additionally, a portion of the infectious individuals succumb to the disease at a rate σ. The immunized or recovered individuals possess temporary immunity, which can wane at a rate φ if they do not have sustained exposure to the infection, causing them to return to the susceptible category.

The mosquito population undergoes a reproductive process, entering the eggs category at a rate denoted as b_{m}. Female mosquitoes deposit their eggs either on water surfaces or in proximity to rivers. However, if the oviposition habitat becomes overcrowded with eggs or lacks sufficient nutrients and water resources, females opt for alternative sites or reduce their egg laying (Bakary et al., 2018). Additionally, larvae and pupae require access to water and nutrients for their development. Therefore, employing the logistic growth concept from Xu et al. (Xu, Zhang, & Zhang, 2016), the per capita oviposition rates for eggs, larvae, and pupae are respectively defined as:

$$b_{\mathrm{m}}\left(1-\frac{E}{K_E}\right)N_{\mathrm{m}}, \quad \tau\left(1-\frac{L}{K_L}\right)E, \quad \text{and} \quad \nu\left(1-\frac{P}{K_P}\right)L, \tag{3}$$

where E represents the number of eggs, L the number of larvae, P the number of pupae, K_E, K_L, and K_P represent the carrying capacities for eggs, larvae, and pupae, respectively, and τ and ν denote the development rates from larvae to pupae and pupae to adult mosquitoes, respectively. The entire mature mosquito population faces a natural mortality rate, represented by η.

When a susceptible mosquito bites either an infectious or a recovered human, it transitions into the category denoted as $E_{\mathrm{m}}(t)$ at rates denoted as κ_1 and κ_2, respectively. Subsequently, after a certain duration, it advances to the infective category, denoted as $I_{\mathrm{m}}(t)$, at a rate χ, where it remains for the rest of its lifespan.

Informed about the disease and control measures through awareness campaigns, individuals can take measures to hinder the development of mosquito eggs, larvae, and pupae, either by employing chemical solutions like insecticides (such as larvicides) or through ecological approaches like cleaning up the environment to reduce the breeding sites for eggs and larvae. The rate at which mosquito variants are eliminated through awareness campaigns is denoted by γ. This rate represents the maximum level of insecticide usage and reflects the impact of awareness campaigns on people's behavior.

2.1.6. Model variables

The variables used in the malaria transmission model are given in Table 1.

2.1.7. Model parameters

The parameters used in the malaria transmission model are given in Table 2, Table 3, and Table 4.

Table 1
Description of model variables.

Variable	Meaning
$S_{\mathrm{ha}}(t)$	Population of Susceptible Aware Humans at time t
$S_{\mathrm{hu}}(t)$	Population of Susceptible Unaware Humans at time t
$S_{\mathrm{m}}(t)$	Population of Susceptible mature mosquitoes at time t
$E_{\mathrm{h}}(t)$	Population of Exposed/Latent Humans at time t
$E_{\mathrm{m}}(t)$	Population of Exposed/Latent mature mosquitoes at time t
$I_{\mathrm{h}}(t)$	Population of Infectious Humans at time t
$I_{\mathrm{m}}(t)$	Population of Infectious mature mosquitoes at time t
$R_{\mathrm{h}}(t)$	Population of Recovered Humans at time t
$R_{\mathrm{m}}(t)$	Population of Recovered mature mosquitoes at time t
$E(t)$	Population of Mosquito eggs in the environment at time t
$L(t)$	Population of Larvae in the environment at time t
$P(t)$	Population of Pupae in the environment at time t
$A(t)$	Level of awareness due to media campaign at time t

Table 2
Description of model parameters in the human population.

Parameter	Meaning
b_h	Growth rate of susceptible unaware human population (either by birth or immigration)
α_1	Rate of awareness by media campaign
α_2	Rate at which aware people become unaware due to negligence
β_1	Rate of disease transmission due to infected mosquito bites
β_2	Rate of disease transmission due to infected mosquito bites
μ	Natural human death rate
σ	Death rate of human due to mosquito bite
λ	Progression rate from E_h to Susceptible due to robust immune system
r	Rate of recovery of the infectious human population due to medication
ρ	Progression rate from E_h to I_h
φ	Per capita rate of loss of immunity in humans
q	Probability of progression from E_h back to S_{ha}
ξ	Probability of progression from R_h back to S_{ha}

Table 3
Description of model parameters in the mosquito population.

Parameter	Meaning
b_m	Rate at which female anopheles mosquitoes lay eggs
η	Natural death rate of mature mosquitoes in the environment
d_E	Natural death rate of mosquito eggs in the environment
d_L	Natural death rate of larvae in the environment
d_P	Natural death rate of pupae in the environment
τ	Progression rate from E stage to L stage
ν	Progression rate from L stage to P stage
ϵ	Progression rate from P stage to susceptible mature mosquito
κ_1	Infection rate of susceptible mosquitoes due to biting infectious humans
κ_2	Infection rate of susceptible mosquitoes due to biting recovered humans
χ	Progression rate from E_m to I_m
γ	Efficacy of insecticide due to the campaign awareness
K_E	Breeder sites occupied by mosquito eggs
K_L	Breeder sites occupied by larvae
K_P	Breeder sites occupied by pupae

Table 4
Description of model parameters in the campaign awareness.

Parameter	Meaning
θ	Rate at which A declines due to fading of memory
δ	Rate at which A increases due to local campaigns
ω	Rate at which A rises due to the campaign through global sources

2.2. The mathematical model

Based on the preceding assumptions and by making a balance of the movements in each compartment, the developed mathematical model for malaria transmission results in a system of twelve first-order ordinary differential equations, as outlined below:

$$\frac{dS_{hu}}{dt} = b_h - \beta_2 S_{hu} I_m + (1-\xi)\varphi R_h - \alpha_1 A S_{hu} + \frac{\alpha_2 S_{ha}}{1+A} + (1-q)\lambda E_h - \mu S_{hu} \tag{4}$$

$$\frac{dS_{ha}}{dt} = -\frac{\beta_1 S_{ha} I_m}{1+A} + \xi\varphi R_h + \alpha_1 A S_{hu} - \frac{\alpha_2 S_{ha}}{1+A} + q\lambda E_h - \mu S_{ha} \tag{5}$$

$$\frac{dE_h}{dt} = \frac{\beta_1 S_{ha} I_m}{1+A} + \beta_2 S_{hu} I_m - (\mu + \lambda + \rho) E_h \tag{6}$$

$$\frac{dI_h}{dt} = \rho E_h - (\mu + \sigma + rA)I_h \tag{7}$$

$$\frac{dR_h}{dt} = rAI_h - (\mu + \varphi)R_h \tag{8}$$

$$\frac{dE}{dt} = b_m\left(1 - \frac{E}{K_E}\right)N_m - (\tau + d_E + \gamma A)E \tag{9}$$

$$\frac{dL}{dt} = \tau\left(1 - \frac{L}{K_L}\right)E - (\nu + d_L + \gamma A)L \tag{10}$$

$$\frac{dP}{dt} = \nu\left(1 - \frac{P}{K_P}\right)L - (\epsilon + d_P + \gamma A)P \tag{11}$$

$$\frac{dS_m}{dt} = \epsilon P - \kappa_1 S_m I_h - \kappa_2 S_m R_h - (\eta + \gamma A)S_m \tag{12}$$

$$\frac{dE_m}{dt} = \kappa_1 S_m I_h + \kappa_2 S_m R_h - (\chi + \eta + \gamma A)E_m \tag{13}$$

$$\frac{dI_m}{dt} = \chi E_m - (\eta + \gamma A)I_m \tag{14}$$

$$\frac{dA}{dt} = \omega I_m + \delta I_h - \theta A \tag{15}$$

Equations (9)–(12) depict the maturation cycle of mosquitoes, while equation (4)–(8), (13), and (14) describe the dynamics of malaria transmission. Equation (15) characterizes the level of awareness campaigns aimed at controlling mosquito vectors of malaria. The initial conditions are:

$$S_{hu}(0) > 0, S_{ha}(0) > 0, E_h(0) > 0, I_h(0) > 0, R_h(0) > 0, E(0) > 0, \tag{16}$$

$$L(0) > 0, P(0) > 0, S_m(0) > 0, E_m(0) > 0, I_m(0) > 0, A(0) > 0. \tag{17}$$

The growth of the entire human population and mature mosquito population is described by the subsequent equations:

$$\frac{dN_h}{dt} = \frac{dS_{hu}}{dt} + \frac{dS_{ha}}{dt} + \frac{dE_h}{dt} + \frac{dI_h}{dt} + \frac{dR_h}{dt} = b_h - \mu N_h - \sigma I_h \tag{18}$$

$$\frac{dN_m}{dt} = \frac{dS_m}{dt} + \frac{dE_m}{dt} + \frac{dI_m}{dt} = \epsilon P - (\eta + \gamma A)N_m \tag{19}$$

The model's behavior is investigated through a combination of dynamical system analysis and numerical simulations.

2.3. Model analysis

In order to improve understanding of the model dynamics, this section presents essential mathematical properties of the model equations.

2.3.1. Existence of disease-free equilibrium points (DFE)

The equilibrium points of interest are derived by solving the model equation (4)–(15) when their left-hand sides are set to zero. To determine the disease-free equilibrium point (DFE), we substitute $I_h = I_m = 0$ into the resulting equations, yielding:

$$S_{hu} = \frac{b_h}{\mu}, S_{ha} = 0, E_h = 0, R_h = 0, E = E^* \tag{20}$$

$$L = L^*, P = P^*, S_m = \frac{\epsilon P^*}{\eta}, E_m = 0, A = 0 \tag{21}$$

Therefore, the DFE is given by $\left(\frac{b_h}{\mu}, 0, 0, 0, 0, E^*, L^*, P^*, \frac{\epsilon P^*}{\eta}, 0, 0, 0\right)$, where

$$E^* = \frac{b_m K_E N_m}{b_m N_m + (\tau + d_E)K_E}, L^* = \frac{\tau K_L E^*}{\tau E^* + (\nu + d_L)K_L}, P^* = \frac{\nu K_P L^*}{\nu L^* + (\epsilon + d_P)K_P} \tag{22}$$

and $N_m = S_m = \frac{\epsilon P^*}{\eta}$. Solving equation (22) simultaneously for E^*, L^* and P^*, with the aid of syms toolkit in MATLAB, we get two solution sets given by

$$(E^*, L^*, P^*) = (0, 0, 0) \tag{23}$$

and

$$(E^*, L^*, P^*) = \left(1 - \frac{1}{R}\right)\left(\frac{K_E}{g_E}, \frac{K_L}{g_L}, \frac{K_P}{g_P}\right) \tag{24}$$

where

$$R = \left(\frac{b_m}{\tau + d_E}\right)\left(\frac{\tau}{\nu + d_L}\right)\left(\frac{\nu}{\epsilon + d_P}\right)\left(\frac{\epsilon}{\eta}\right) \tag{25}$$

$$g_E = \left[1 + \frac{(d_E + \tau)(K_P d_P + K_P \epsilon + K_L \nu)\eta K_E}{K_L K_P b_m \epsilon \nu}\right] \tag{26}$$

$$g_L = \left[1 + \frac{(d_L + \nu)(K_P b_m \epsilon + K_E d_E \eta + K_E \eta \tau)K_L}{K_E K_P b_m \epsilon \tau}\right] \tag{27}$$

$$g_P = \left[1 + \frac{(d_P + \epsilon)(K_L d_L + K_L \nu + K_E \tau)K_P}{K_E K_L \nu \tau}\right] \tag{28}$$

The threshold quantity R is called regulatory threshold parameter of the mosquito population. If $R \leq 1$, then the model does not possess any equilibrium aside from the trivial disease-free equilibrium point defined as:

$$(S_{hu}^*, S_{ha}^*, E_h^*, I_h^*, R_h^*, E^*, L^*, P^*, S_m^*, E_m^*, I_m^*, A^*) = \left(\frac{b_h}{\mu}, 0, 0, 0, 0, 0, 0, 0, 0, 0, 0, 0\right) \tag{29}$$

If $R > 1$, then the model has a non-trivial disease-free equilibrium point given by

$$\left(\frac{b_h}{\mu}, 0, 0, 0, 0, E^*, L^*, P^*, \frac{\epsilon P^*}{\eta}, 0, 0, 0\right) \tag{30}$$

where E^*, L^* and P^* are given by equation (24). We will exclusively focus on the nontrivial equilibrium point (30) as it aligns more closely with biological realism. Therefore, for the remainder of the paper, we consider the case $R > 1$.

2.3.2. Jacobian matrix and stability analysis of DFE

The Jacobian matrix of the model is given by

$$\mathbf{J} = \begin{bmatrix} \frac{\partial S'_{hu}}{\partial S_{hu}} & \frac{\partial S'_{hu}}{\partial S_{ha}} & \frac{\partial S'_{hu}}{\partial E_h} & \frac{\partial S'_{hu}}{\partial I_h} & \frac{\partial S'_{hu}}{\partial R_h} & \frac{\partial S'_{hu}}{\partial E} & \frac{\partial S'_{hu}}{\partial L} & \frac{\partial S'_{hu}}{\partial P} & \frac{\partial S'_{hu}}{\partial S_m} & \frac{\partial S'_{hu}}{\partial E_m} & \frac{\partial S'_{hu}}{\partial I_m} & \frac{\partial S'_{hu}}{\partial A} \\ \frac{\partial S'_{ha}}{\partial S_{hu}} & \frac{\partial S'_{ha}}{\partial S_{ha}} & \frac{\partial S'_{ha}}{\partial E_h} & \frac{\partial S'_{ha}}{\partial I_h} & \frac{\partial S'_{ha}}{\partial R_h} & \frac{\partial S'_{ha}}{\partial E} & \frac{\partial S'_{ha}}{\partial L} & \frac{\partial S'_{ha}}{\partial P} & \frac{\partial S'_{ha}}{\partial S_m} & \frac{\partial S'_{ha}}{\partial E_m} & \frac{\partial S'_{ha}}{\partial I_m} & \frac{\partial S'_{ha}}{\partial A} \\ \frac{\partial E'_h}{\partial S_{hu}} & \frac{\partial E'_h}{\partial S_{ha}} & \frac{\partial E'_h}{\partial E_h} & \frac{\partial E'_h}{\partial I_h} & \frac{\partial E'_h}{\partial R_h} & \frac{\partial E'_h}{\partial E} & \frac{\partial E'_h}{\partial L} & \frac{\partial E'_h}{\partial P} & \frac{\partial E'_h}{\partial S_m} & \frac{\partial E'_h}{\partial E_m} & \frac{\partial E'_h}{\partial I_m} & \frac{\partial E'_h}{\partial A} \\ \frac{\partial I'_h}{\partial S_{hu}} & \frac{\partial I'_h}{\partial S_{ha}} & \frac{\partial I'_h}{\partial E_h} & \frac{\partial I'_h}{\partial I_h} & \frac{\partial I'_h}{\partial R_h} & \frac{\partial I'_h}{\partial E} & \frac{\partial I'_h}{\partial L} & \frac{\partial I'_h}{\partial P} & \frac{\partial I'_h}{\partial S_m} & \frac{\partial I'_h}{\partial E_m} & \frac{\partial I'_h}{\partial I_m} & \frac{\partial I'_h}{\partial A} \\ \frac{\partial R'_h}{\partial S_{hu}} & \frac{\partial R'_h}{\partial S_{ha}} & \frac{\partial R'_h}{\partial E_h} & \frac{\partial R'_h}{\partial I_h} & \frac{\partial R'_h}{\partial R_h} & \frac{\partial R'_h}{\partial E} & \frac{\partial R'_h}{\partial L} & \frac{\partial R'_h}{\partial P} & \frac{\partial R'_h}{\partial S_m} & \frac{\partial R'_h}{\partial E_m} & \frac{\partial R'_h}{\partial I_m} & \frac{\partial R'_h}{\partial A} \\ \frac{\partial E'}{\partial S_{hu}} & \frac{\partial E'}{\partial S_{ha}} & \frac{\partial E'}{\partial E_h} & \frac{\partial E'}{\partial I_h} & \frac{\partial E'}{\partial R_h} & \frac{\partial E'}{\partial E} & \frac{\partial E'}{\partial L} & \frac{\partial E'}{\partial P} & \frac{\partial E'}{\partial S_m} & \frac{\partial E'}{\partial E_m} & \frac{\partial E'}{\partial I_m} & \frac{\partial E'}{\partial A} \\ \frac{\partial L'}{\partial S_{hu}} & \frac{\partial L'}{\partial S_{ha}} & \frac{\partial L'}{\partial E_h} & \frac{\partial L'}{\partial I_h} & \frac{\partial L'}{\partial R_h} & \frac{\partial L'}{\partial E} & \frac{\partial L'}{\partial L} & \frac{\partial L'}{\partial P} & \frac{\partial L'}{\partial S_m} & \frac{\partial L'}{\partial E_m} & \frac{\partial L'}{\partial I_m} & \frac{\partial L'}{\partial A} \\ \frac{\partial P'}{\partial S_{hu}} & \frac{\partial P'}{\partial S_{ha}} & \frac{\partial P'}{\partial E_h} & \frac{\partial P'}{\partial I_h} & \frac{\partial P'}{\partial R_h} & \frac{\partial P'}{\partial E} & \frac{\partial P'}{\partial L} & \frac{\partial P'}{\partial P} & \frac{\partial P'}{\partial S_m} & \frac{\partial P'}{\partial E_m} & \frac{\partial P'}{\partial I_m} & \frac{\partial P'}{\partial A} \\ \frac{\partial S'_m}{\partial S_{hu}} & \frac{\partial S'_m}{\partial S_{ha}} & \frac{\partial S'_m}{\partial E_h} & \frac{\partial S'_m}{\partial I_h} & \frac{\partial S'_m}{\partial R_h} & \frac{\partial S'_m}{\partial E} & \frac{\partial S'_m}{\partial L} & \frac{\partial S'_m}{\partial P} & \frac{\partial S'_m}{\partial S_m} & \frac{\partial S'_m}{\partial E_m} & \frac{\partial S'_m}{\partial I_m} & \frac{\partial S'_m}{\partial A} \\ \frac{\partial E'_m}{\partial S_{hu}} & \frac{\partial E'_m}{\partial S_{ha}} & \frac{\partial E'_m}{\partial E_h} & \frac{\partial E'_m}{\partial I_h} & \frac{\partial E'_m}{\partial R_h} & \frac{\partial E'_m}{\partial E} & \frac{\partial E'_m}{\partial L} & \frac{\partial E'_m}{\partial P} & \frac{\partial E'_m}{\partial S_m} & \frac{\partial E'_m}{\partial E_m} & \frac{\partial E'_m}{\partial I_m} & \frac{\partial E'_m}{\partial A} \\ \frac{\partial I'_m}{\partial S_{hu}} & \frac{\partial I'_m}{\partial S_{ha}} & \frac{\partial I'_m}{\partial E_h} & \frac{\partial I'_m}{\partial I_h} & \frac{\partial I'_m}{\partial R_h} & \frac{\partial I'_m}{\partial E} & \frac{\partial I'_m}{\partial L} & \frac{\partial I'_m}{\partial P} & \frac{\partial I'_m}{\partial S_m} & \frac{\partial I'_m}{\partial E_m} & \frac{\partial I'_m}{\partial I_m} & \frac{\partial I'_m}{\partial A} \\ \frac{\partial A'}{\partial S_{hu}} & \frac{\partial A'}{\partial S_{ha}} & \frac{\partial A'}{\partial E_h} & \frac{\partial A'}{\partial I_h} & \frac{\partial A'}{\partial R_h} & \frac{\partial A'}{\partial E} & \frac{\partial A'}{\partial L} & \frac{\partial A'}{\partial P} & \frac{\partial A'}{\partial S_m} & \frac{\partial A'}{\partial E_m} & \frac{\partial A'}{\partial I_m} & \frac{\partial A'}{\partial A} \end{bmatrix} \tag{31}$$

or

$$\mathbf{J} = \begin{bmatrix} \mathbf{J}_{11} & \mathbf{J}_{12} \\ \mathbf{J}_{21} & \mathbf{J}_{22} \end{bmatrix} \tag{32}$$

where

$$\mathbf{J}_{11} = \begin{bmatrix} -(\beta_2 I_m + \alpha_1 A + \mu) & \frac{\alpha_2}{1+A} & (1-q)\lambda & 0 & (1-\xi)\varphi \\ \alpha_1 A & -\left(\frac{\beta_1 I_m}{1+A} + \frac{\alpha_2}{1+A} + \mu\right) & q\lambda & 0 & \xi\varphi \\ \beta_2 I_m & \frac{\beta_1 I_m}{1+A} & -(\mu+\lambda+\rho) & 0 & 0 \\ 0 & 0 & \rho & -(\mu+\sigma+rA) & 0 \end{bmatrix} \tag{33}$$

$$\mathbf{J}_{12} = \begin{bmatrix} 0 & 0 & 0 & 0 & 0 & -\beta_2 S_{\mathrm{hu}} & -\left(\alpha_1 S_{\mathrm{hu}} + \dfrac{\alpha_2 S_{\mathrm{ha}}}{(1+A)^2}\right) \\ 0 & 0 & 0 & 0 & 0 & -\dfrac{\beta_1 S_{\mathrm{ha}}}{1+A} & \dfrac{\beta_1 S_{\mathrm{ha}} I_{\mathrm{m}}}{(1+A)^2} + \alpha_1 S_{\mathrm{hu}} + \dfrac{\alpha_2 S_{\mathrm{ha}}}{(1+A)^2} \\ 0 & 0 & 0 & 0 & 0 & \dfrac{\beta_1 S_{\mathrm{ha}}}{1+A} + \beta_2 S_{\mathrm{hu}} & 0 \\ 0 & 0 & 0 & 0 & 0 & 0 & 0 \end{bmatrix} \tag{34}$$

$$\mathbf{J}_{21} = \begin{bmatrix} 0 & 0 & 0 & rA & -(\mu+\varphi) \\ 0 & 0 & 0 & 0 & 0 \\ 0 & 0 & 0 & 0 & 0 \\ 0 & 0 & 0 & 0 & 0 \\ 0 & 0 & 0 & -\kappa_1 S_{\mathrm{m}} & -\kappa_2 S_{\mathrm{m}} \\ 0 & 0 & 0 & \kappa_1 S_{\mathrm{m}} & \kappa_2 S_{\mathrm{m}} \\ 0 & 0 & 0 & 0 & 0 \\ 0 & 0 & 0 & \delta & 0 \end{bmatrix} \tag{35}$$

and $\mathbf{J}_{22} = [\mathbf{J}_{22A} \quad \mathbf{J}_{22B}]$; where

$$\mathbf{J}_{22A} = \begin{bmatrix} 0 & 0 & 0 & 0 \\ -\dfrac{b_{\mathrm{m}} N_{\mathrm{m}}}{K_E} - (\tau + d_E + \gamma A) & 0 & 0 & b_{\mathrm{m}}\left(1 - \dfrac{E}{K_E}\right) \\ \tau\left(1 - \dfrac{L}{K_L}\right) & -\dfrac{\tau E}{K_L} - (\nu + d_L + \gamma A) & 0 & 0 \\ 0 & \nu\left(1 - \dfrac{P}{K_P}\right) & -\left(\dfrac{\nu L}{K_P} + \epsilon + d_P + \gamma A\right) & 0 \\ 0 & 0 & \epsilon & -(\kappa_1 I_{\mathrm{h}} + \kappa_2 R_{\mathrm{h}} + \eta + \gamma A) \\ 0 & 0 & 0 & (\kappa_1 I_{\mathrm{h}} + \kappa_2 R_{\mathrm{h}}) \\ 0 & 0 & 0 & 0 \\ 0 & 0 & 0 & 0 \end{bmatrix} \tag{36}$$

$$\mathbf{J}_{22B} = \begin{bmatrix} 0 & 0 & 0 \\ b_{\mathrm{m}}\left(1 - \dfrac{E}{K_E}\right) & b_{\mathrm{m}}\left(1 - \dfrac{E}{K_E}\right) & -\gamma E \\ 0 & 0 & -\gamma L \\ 0 & 0 & -\gamma P \\ 0 & 0 & -\gamma S_{\mathrm{m}} \\ -(\chi + \eta + \gamma A) & 0 & -\gamma E_{\mathrm{m}} \\ \chi & -(\eta + \gamma A) & -\gamma I_{\mathrm{m}} \\ 0 & \omega & -\theta \end{bmatrix} \tag{37}$$

Evaluating $\mathbf{J}$ at the DFE given by equation (30) yields the matrix

$$\mathbf{A} = \mathbf{J}(DFE) = [\,\mathbf{A}_{11} \quad \mathbf{A}_{12}\,] \tag{38}$$

where

$$\mathbf{A}_{11} = \begin{bmatrix} -\mu & \alpha_2 & (1-q)\lambda & 0 & (1-\xi)\varphi & 0 \\ 0 & -(\alpha_2+\mu) & q\lambda & 0 & \xi\varphi & 0 \\ 0 & 0 & -(\mu+\lambda+\rho) & 0 & 0 & 0 \\ 0 & 0 & \rho & -(\mu+\sigma) & 0 & 0 \\ 0 & 0 & 0 & 0 & -(\mu+\varphi) & 0 \\ 0 & 0 & 0 & 0 & 0 & -\dfrac{b_{\mathrm{m}}N_{\mathrm{m}}^*}{K_E} - (\tau + d_E) \\ 0 & 0 & 0 & 0 & 0 & \tau\left(1 - \dfrac{L^*}{K_L}\right) \\ 0 & 0 & 0 & 0 & 0 & 0 \\ 0 & 0 & 0 & -\kappa_1 S_{\mathrm{m}}^* & -\kappa_2 S_{\mathrm{m}}^* & 0 \\ 0 & 0 & 0 & \kappa_1 S_{\mathrm{m}}^* & \kappa_2 S_{\mathrm{m}}^* & 0 \\ 0 & 0 & 0 & 0 & 0 & 0 \\ 0 & 0 & 0 & \delta & 0 & 0 \end{bmatrix} \tag{39}$$

$$\mathbf{A}_{12} = \begin{bmatrix} 0 & 0 & 0 & 0 & -\beta_2 S_{\mathrm{hu}}^* & -\alpha_1 S_{\mathrm{hu}}^* \\ 0 & 0 & 0 & 0 & 0 & \alpha_1 S_{\mathrm{hu}}^* \\ 0 & 0 & 0 & 0 & \beta_2 S_{\mathrm{hu}}^* & 0 \\ 0 & 0 & 0 & 0 & 0 & 0 \\ 0 & 0 & 0 & 0 & 0 & 0 \\ 0 & 0 & b_{\mathrm{m}}\left(1 - \dfrac{E^*}{K_E}\right) & b_{\mathrm{m}}\left(1 - \dfrac{E^*}{K_E}\right) & b_{\mathrm{m}}\left(1 - \dfrac{E^*}{K_E}\right) & -\gamma E^* \\ -\left(\dfrac{\tau E^*}{K_L} + \nu + d_L\right) & 0 & 0 & 0 & 0 & -\gamma L^* \\ \nu\left(1 - \dfrac{P^*}{K_P}\right) & -\left(\dfrac{\nu L^*}{K_P} + \epsilon + d_P\right) & 0 & 0 & 0 & -\gamma P^* \\ 0 & \epsilon & -\eta & 0 & 0 & -\gamma S_{\mathrm{m}}^* \\ 0 & 0 & 0 & -(\chi+\eta) & 0 & 0 \\ 0 & 0 & 0 & \chi & -\eta & 0 \\ 0 & 0 & 0 & 0 & \omega & -\theta \end{bmatrix} \tag{40}$$

Here, $S_{\mathrm{hu}}^* = \frac{b_{\mathrm{h}}}{\mu}, N_{\mathrm{m}}^* = S_{\mathrm{m}}^* = \frac{\epsilon P^*}{\eta}$, while E^*, L^* and P^* are given by equation (24). Using eig built-in function in MATLAB, we found that all the eigenvalues of $\mathbf{A}$ are either negatives or have negative real part. Hence, the DFE given by equation (30) is locally asymptotically stable.

2.3.3. Basic reproduction number

The basic reproduction number, denoted by R_0, is the number of secondary infections that are produced by one primary infection in a completely susceptible population at a disease-free equilibrium (DFE). It serves as a pivotal threshold, signifying whether the disease can persist in the population or die out. To compute R_0 for the model, we employ the next-generation matrix technique, as outlined in (Van den Driessche & James, 2002).

Considering only the equations for the "diseased" classes, let $\mathbf{X} = [E_h, I_h, R_h, E_m, I_m]^T$. Thus, the model can be written as:

$$\frac{d\mathbf{X}}{dt} = F(\mathbf{X}) - V(\mathbf{X}), \tag{41}$$

where $F(\mathbf{X})$ and $V(\mathbf{X})$ are column vectors given by

$$F(\mathbf{X}) = \begin{bmatrix} \frac{\beta_1 S_{ha} I_m}{1+A} + \beta_2 S_{hu} I_m \\ 0 \\ 0 \\ \kappa_1 S_m I_h + \kappa_2 S_m R_h \\ 0 \end{bmatrix} \text{ and } V(\mathbf{X}) = \begin{bmatrix} (\mu+\lambda+\rho)E_h \\ -\rho E_h + (\mu+\sigma+rA)I_h \\ -rAI_h + (\mu+\varphi)R_h \\ (\chi+\eta+\gamma A)E_m \\ -\chi E_m + (\eta+\gamma A)I_m \end{bmatrix} \tag{42}$$

Let

$$\mathbf{f} = \begin{bmatrix} \frac{\partial F}{\partial E_h} & \frac{\partial F}{\partial I_h} & \frac{\partial F}{\partial R_h} & \frac{\partial F}{\partial E_m} & \frac{\partial F}{\partial I_m} \end{bmatrix}, \mathbf{v} = \begin{bmatrix} \frac{\partial V}{\partial E_h} & \frac{\partial V}{\partial I_h} & \frac{\partial V}{\partial R_h} & \frac{\partial V}{\partial E_m} & \frac{\partial V}{\partial I_m} \end{bmatrix} \tag{43}$$

Evaluating **f** and **v** at the disease-free equilibrium (DFE) point, obtained above, yields

$$\mathbf{f} = \begin{bmatrix} 0 & 0 & 0 & 0 & \beta_2 S_{hu}^* \\ 0 & 0 & 0 & 0 & 0 \\ 0 & 0 & 0 & 0 & 0 \\ 0 & \kappa_1 S_m^* & \kappa_2 S_m^* & 0 & 0 \\ 0 & 0 & 0 & 0 & 0 \end{bmatrix} \tag{44}$$

$$\mathbf{v} = \begin{bmatrix} (\mu+\lambda+\rho) & 0 & 0 & 0 & 0 \\ -\rho & (\mu+\sigma) & 0 & 0 & 0 \\ 0 & 0 & (\mu+\varphi) & 0 & 0 \\ 0 & 0 & 0 & (\chi+\eta) & 0 \\ 0 & 0 & 0 & -\chi & \eta \end{bmatrix} \tag{45}$$

Here, $S_{hu}^* = \frac{b_h}{\mu}$ and $S_m^* = \frac{\epsilon P^*}{\eta}$. The associated next generation matrix is given by $\mathbf{G} = \mathbf{f}^*\mathbf{v}^{-1}$, i.e.,

$$\mathbf{G} = \begin{bmatrix} 0 & 0 & 0 & \frac{b_h \beta_2 \chi}{\eta\mu(\chi+\eta)} & \frac{b_h \beta_2}{\eta\mu} \\ 0 & 0 & 0 & 0 & 0 \\ 0 & 0 & 0 & 0 & 0 \\ \frac{P^* \epsilon \kappa_1 \rho}{\eta(\mu+\sigma)(\lambda+\mu+\rho)} & \frac{P^* \epsilon \kappa_1}{\eta(\mu+\sigma)} & \frac{P^* \epsilon \kappa_2}{\eta(\mu+varphi)} & 0 & 0 \\ 0 & 0 & 0 & 0 & 0 \end{bmatrix} \tag{46}$$

Hence, we obtain R_0 as the largest magnitude eigenvalue of **G** (or the spectral radius of **G**) given by

$$R_0 = \frac{1}{\eta}\sqrt{\frac{P^* b_h \beta_2 \chi \epsilon \kappa_1 \rho}{\mu(\chi+\eta)(\mu+\sigma)(\lambda+\mu+\rho)}} \tag{47}$$

where P^* is given by equation (24). In Section 3, we will employ the model equation (4)–(15) in conjunction with data from Kenya to analyze the malaria dynamics and, subsequently, identify conditions for potential disease eradication.

3. Numerical simulation: a case study of malaria incidence in Kenya

In this section, numerical simulations are considered to explore the dynamics of model equation (4)–(15) so as to predict the future trend of the disease and explore the control measures. We estimate solutions to the model equations by employing fourth and fifth-order Runge-Kutta techniques, which are executed through the ode45 built-in function in MATLAB. The initial values of the model variables are taken as follows:

$$S_{\mathrm{hu}}(0) = 15000, S_{\mathrm{ha}}(0) = 0, E_{\mathrm{h}}(0) = 1250, I_{\mathrm{h}}(0) = 221.6 R_{\mathrm{h}}(0) = 0, E(0) = 2400 \tag{48}$$

$$L(0) = 800, P(0) = 400, S_{\mathrm{m}}(0) = 300, I_{\mathrm{m}}(0) = 50, E_{\mathrm{m}}(0) = 30, A(0) = 0 \tag{49}$$

The initial parameter guesses are taken as: $\beta_1 = 0.0044$, $\beta_2 = 0.001$, $\alpha_1 = 0.04$, $\alpha_2 = 0.5$, $\tau = 0.03$, $\chi = 0.005$, $\kappa_1 = 0.001$, $\kappa_2 = 0.03$, $\epsilon = 0.002$, $\nu = 0.005$, $\varphi = 0.005$, $\rho = 0.004$, $\lambda = 0.5$, $r = 1/14$, $q = 0.8$, $\xi = 0.9$, $\sigma = 0.0028$, $\gamma = 0.003$, $\omega = 0.1$, $\theta = 0.01$, $\delta = 0.015$, and $b_{\mathrm{m}} = 1$.

3.1. Model fitting

The model was fitted and its parameters were estimated using the actual data on incidence of malaria (per 1000 population at risk) in Kenya from 2000 to 2021, obtained from The World Bank (World Bank, 2021). The transmission rates β_1 and β_2 from mosquito bites were multiplied by a seasonality factor given by

$$s(t) = \left(1 + \cos\left(\frac{\pi}{15}t\right)\right) \tag{50}$$

to account for irregular seasonal patterns in the data (Herdicho et al., 2021). The model was fitted to the total infected human population. The fitting algorithm was the least-squares curve fitting using the built-in lsqcurvefit function in MATLAB from the optimization toolbox. To mitigate the potential for overfitting, we conducted a series of additional analyses.

1. Cross-validation: We employed k-fold cross-validation to evaluate the model's generalization ability. The data was partitioned into k folds, and the model was trained on k-1 folds, with its performance assessed on the remaining fold. This process was repeated k times, and the average performance across all folds served as an estimate of the model's generalization performance.
2. Regularization: To curb the model's complexity and prevent overfitting, regularization techniques, such as L_1 and L_2 regularization, were applied. Regularization imposes a penalty on large parameter values, effectively making the model more resistant to noise in the data.
3. Early stopping: Early stopping was implemented to prevent excessive training and overfitting. During training, the model's performance on a validation set was monitored, and training was halted when the validation set performance began to decline.

These analyses provided additional evidence that the model is not overfitting the data. The cross-validation results suggest that the model generalizes well to new data. The regularization techniques and early stopping procedures help to ensure that the model is not overly complex and does not overfit the training data. The computer simulations were done in MATLAB software to obtain the profiles of the model variables. The fitting algorithm yielded a mean absolute error (MAE) of 2.6463 when comparing the actual data points to the simulated values of infectious human population (I_{h}). This finding indicates that the proposed mathematical model closely aligns with the recorded malaria incidence data in Kenya.

3.2. Parameter optimization

Optimized numerical values of the model parameters are given in Table 5. Parameters that relate to the various rates and probabilities were estimated using the fitting algorithm. The unit of most of the parameter values in Table 5 are in per day, but they were converted to per year in the numerical simulations to suit our time scale in the study.

The life expectancy of human, mature mosquitoes, mosquito eggs, larvae and pupae in Kenya are given in Table 6.

Table 5
Numerical values of the model parameters.

Parameter	Unit	Value	Source
b_h	Humans/day	90	Assumed
α_1	day^{-1}	0.001005	Estimated
α_2	day^{-1}	0.003642	Estimated
β_1	day^{-1}	0.541938	Estimated
β_2	day^{-1}	0.006162	Estimated
μ	day^{-1}	4.0891×10^{-5}	Computed from Table 6
σ	day^{-1}	0.107504	Estimated
λ	day^{-1}	0.115671	Estimated
r	day^{-1}	0.111606	Estimated
ρ	day^{-1}	0.064952	Estimated
φ	day^{-1}	0.374557	Estimated
q	Dimensionless	0.001910	Estimated
ξ	Dimensionless	0.001000	Estimated
b_m	Dimensionless	12.797272	Estimated
η	day^{-1}	0.011111	Computed from Table 6
d_E	day^{-1}	0.028571	Computed from Table 6
d_L	day^{-1}	0.071429	Computed from Table 6
d_P	day^{-1}	0.033333	Computed from Table 6
τ	day^{-1}	0.465955	Estimated
ν	day^{-1}	0.709890	Estimated
ϵ	day^{-1}	0.254144	Estimated
κ_1	day^{-1}	0.001743	Estimated
κ_2	day^{-1}	0.010966	Estimated
χ	day^{-1}	0.061551	Estimated
γ	day^{-1}	0.441291	Estimated
K_E	Space	1.5×10^4	Traoré et al. (Traor et al., 2017)
K_L	Space	1.0×10^4	Traoré et al. (Traor et al., 2017)
K_P	Space	7.0×10^3	Traoré et al. (Traor et al., 2017)
θ	day^{-1}	0.116657	Estimated
δ	day^{-1}	0.004381	Estimated
ω	day^{-1}	0.146587	Estimated

Table 6
Life expectancy of human hosts and mosquito vectors.

Parameter	Description	Unit	Value	Source
$\frac{1}{\mu}$	Life expectancy of humans	days	24,455	WHO (World Health Organization, 2023)
$\frac{1}{\mu_l}$	Life expectancy of mature mosquitoes	days	90	WHO (World Health Organization, 2023)
$\frac{1}{\eta}$	Life expectancy of mosquito eggs	days	35	WHO (World Health Organization, 2023)
$\frac{1}{d_E}$	Life expectancy of larvae	days	14	WHO (World Health Organization, 2023)
$\frac{1}{d_L}$	Life expectancy of pupae	days	30	WHO (World Health Organization, 2023)
$\frac{1}{d_P}$				

4. Results and discussion

Employing the estimated parameter values presented in Table 5, we calculated the basic reproduction number (R_0) to be 2.4537. This indicates that without stringent adherence to control measures, malaria infections will persist within the human population in Kenya. This finding corroborates the findings of previous surveillance reports by the World Health Organization (WHO) that malaria is endemic in Kenya (World Health Organization, 2023).

4.1. Validation of the model

Model fitting results are presented in Fig. 2. The analysis yielded a mean absolute error (MAE) of 2.6463 when comparing the observed data points to the simulated values of I_h. These findings indicate that the proposed mathematical model closely aligns with the recorded malaria incidence in Kenya from 2000 to 2021. Consequently, the model can be employed to generate future predictions of malaria transmission dynamics in Kenya.

4.2. The simulated human and mosquito populations

Utilizing the estimated parameter values presented in Table 5, the potential long-term dynamics of malaria in Kenya from 2000 to 2030 are depicted in Fig. 3. The simulation outcome illustrated in Fig. 3 (c) demonstrates that the prevalence of malaria in Kenya consistently fluctuates between 30 and 300 cases per 1000 individuals at risk of infection. This suggests that

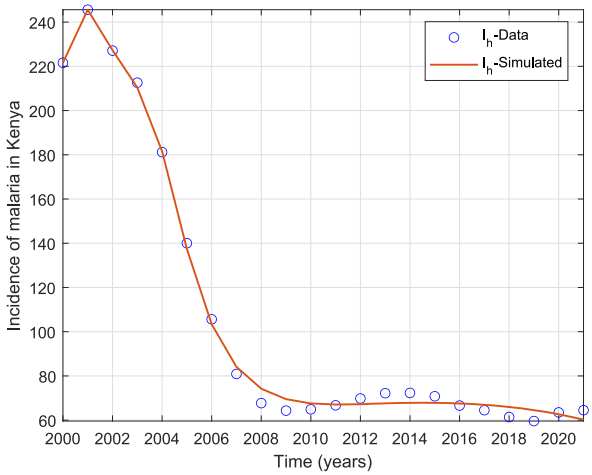

Fig. 2. Model fit of the incidence of malaria per 1000 population at risk in Kenya from 2000 to 2021.

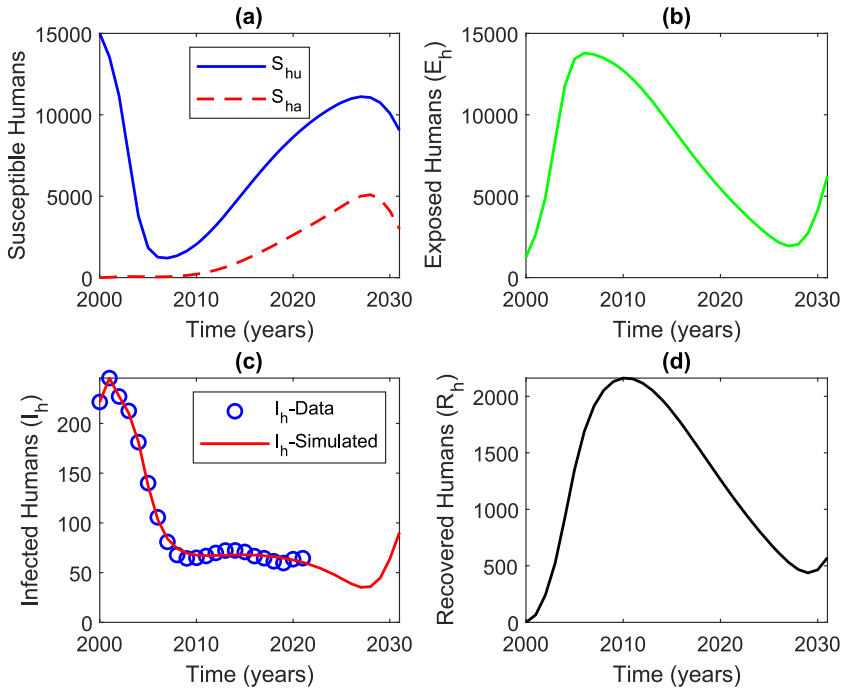

Fig. 3. Plot showing a possible long-term dynamics of malaria transmission in Kenya between 2000 and 2030.

in the absence of more effective control measures, malaria is likely to persist as an endemic disease in Kenya for an extended period.

The dynamics of the mosquito population in Kenya from 2000 to 2030 are illustrated in Fig. 4. The results indicate that malaria vector mosquitoes are likely to persist and thrive in the Kenyan environment beyond 2030.

4.3. Impact of awareness campaign on the model's dynamical behavior

The impact of awareness campaigns on malaria incidence in Kenya is depicted in Fig. 5. The figure clearly illustrates a significant reduction in malaria incidence as the level of campaign awareness increases. This inverse relationship is characterized by a fluctuating pattern, suggesting that sustained and intensified awareness campaigns could potentially drive down malaria cases to as low as 40.

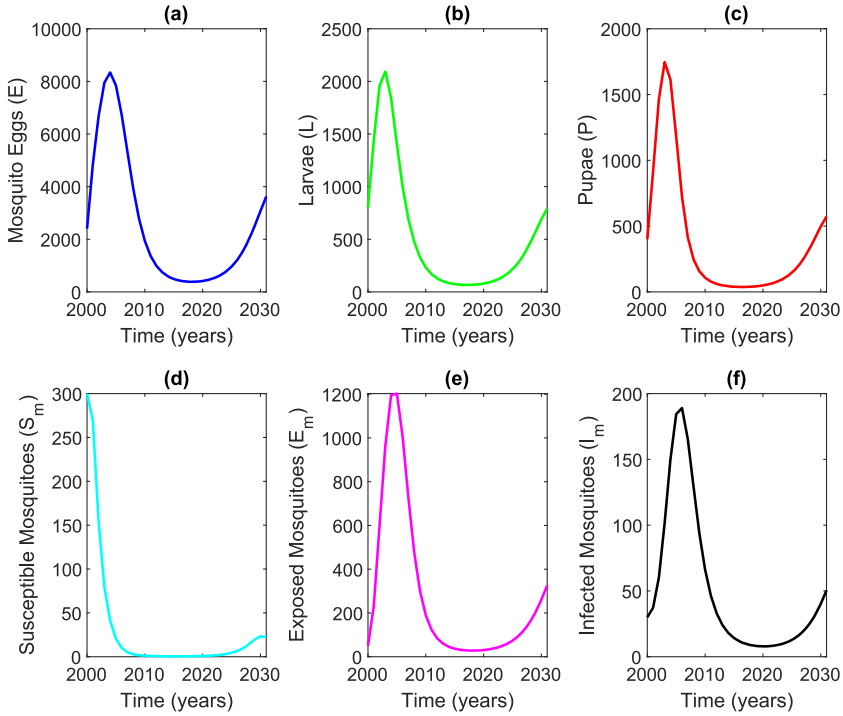

Fig. 4. Plot showing a possible long-term trend of mosquito population in Kenya between 2000 and 2030.

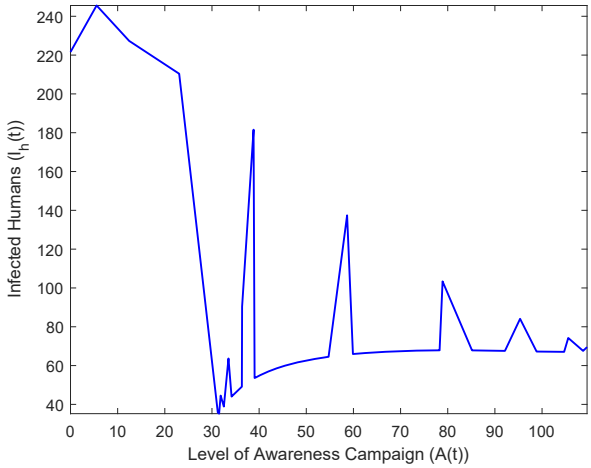

Fig. 5. Plot showing the effects of awareness campaign on the dynamics of infected humans in Kenya between 2000 and 2030.

Fig. 6 illustrates the impact of awareness campaigns on mosquito populations in Kenya. The figure reveals a fluctuating pattern, suggesting that as campaign awareness levels increase, there is a noticeable decrease in mosquito variants. However, it is crucial to acknowledge that the long-term eradication of all mosquito vectors remains elusive without the implementation of more effective control measures than those currently in place.

5. Summary and conclusions

Mathematical modeling has emerged as a powerful tool for unraveling the intricacies of seasonal malaria transmission patterns and guiding effective control strategies. In this study, we employ a deterministic model to delve into the transmission dynamics of malaria in Kenya. Our comprehensive model incorporates various factors that significantly influence malaria transmission, including mosquito behavior, seasonality, and awareness-based interventions. We meticulously calibrated the

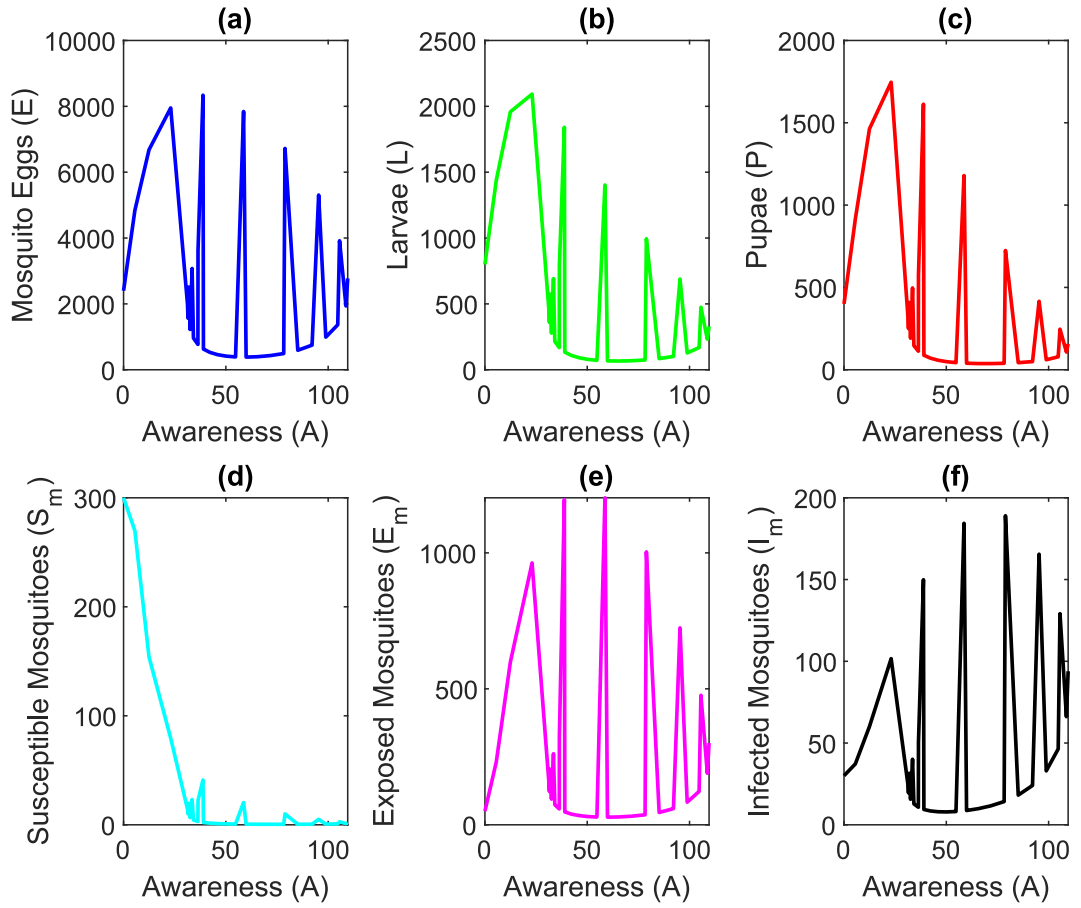

Fig. 6. Plot showing the effects of level of awareness campaign on the dynamics of mosquitoes in Kenya between 2000 and 2030.

model to encompass malaria incidence data from Kenya between 2000 and 2021 using least squares curve fitting. The model parameters were then estimated from the fitting algorithm, enabling us to forecast disease dynamics up to the year 2030.

Our study confirms that the model accurately reflects the observed data and reveals that the dynamics of immature mosquitoes play a pivotal role in shaping malaria transmission. Notably, malaria transmission is profoundly influenced by the regulatory threshold parameter (R) of the mosquito population and the basic reproduction number (R_0). As these threshold quantities increase, so does the severity of malaria outbreaks. Therefore, incorporating the life cycle of Anopheles mosquitoes into malaria modeling is crucial for generating accurate predictions and designing effective control strategies.

Furthermore, our findings demonstrate that effectively managing malaria transmission hinges on actively controlling mosquito population growth. This can be achieved through targeted awareness campaigns that aim to reduce the availability of mosquito breeding sites (K_E, K_L, and K_P). However, it is important to acknowledge a limitation of our model: it was specifically designed to investigate the dynamics of malaria transmission and does not explicitly account for the potential impact of climate change on mosquito life cycles.

To maximize the impact of malaria control efforts, tailored social media campaigns should be targeted towards specific populations, ensuring that messaging is relevant and culturally sensitive. Additionally, optimization control measures should be employed to strategically allocate resources and interventions, ensuring that they are deployed in the most effective and efficient manner possible. Finally, integrating effective management methods, such as insecticide-treated bed nets and indoor residual spraying, into comprehensive malaria control strategies is essential for reducing malaria transmission and protecting public health.

6. Future research

Future research endeavors should continue to delve into innovative modeling approaches to tackle the ever-evolving challenges posed by malaria transmission. This includes addressing critical factors such as.

(i) Drug resistance, which has emerged as a significant threat to malaria control efforts and warrants careful investigation within the context of modeling studies.
(ii) Time-dependent model parameters, which should be incorporated to capture the dynamic nature of malaria transmission and account for fluctuations in environmental factors and human behavior.
(iii) The degree of vulnerability of human populations, which varies across geographical regions and demographic groups. Understanding these variations is crucial for designing targeted interventions that effectively protect the most susceptible individuals.
(iv) Integration of genetic and genomic data, which can provide valuable insights into the mechanisms of drug resistance, parasite evolution, and vector-host interactions. This integration can lead to more accurate and predictive models.
(v) Incorporating the influence of climate change on the mosquito life cycle, which has the potential to alter parasite distribution, abundance, and transmission patterns. Understanding these complex interactions is essential for anticipating and mitigating the impact of climate change on malaria epidemiology.

Additionally, the development of spatially explicit models can help tailor interventions to specific geographical areas, optimizing resource allocation and maximizing the effectiveness of control strategies.

Data availability

The original data on incidence of malaria (per 1000 population at risk) in Kenya from 2000 to 2021 is available at The World Bank (World Bank, 2021). The MATLAB® source code used to support the findings of this study are available from the corresponding author upon request. The code was generated by MATLAB® software version R2021a (9.10.0.1602886).

Funding

This study has not received any funding.

CRediT authorship contribution statement

Francis Oketch Ochieng: Conceptualization, Data curation, Formal analysis, Investigation, Methodology, Project administration, Software, Validation, Visualization, Writing – original draft, Writing – review & editing.

Declaration of competing interest

The author affirms that there are no conflicts of interest concerning the research, authorship, or publication of this paper. Hence, the publisher is free to proceed with publishing this paper following the review process.

References

Bakary, T., Boureima, S., & Sado, T. (2018). A mathematical model of malaria transmission in a periodic environment. In *Journal of biological dynamics* (Vol. 12, pp. 400–432), 1.
Basir, F. Al, & Abraha, T. (2023). Mathematical modelling and optimal control of malaria using awareness-based interventions. In *Mathematics* (Vol. 11, p. 1687), 7.
Centers for disease control and prevention. *Malaria*, (2023). https://www.cdc.gov/malaria/index.html. (Accessed 15 September 2023).
Chitnis, N., et al. (2010). Comparing the effectiveness of malaria vector-control interventions through a mathematical model. In *The American journal of tropical medicine and hygiene* (Vol. 83, p. 230), 2.
Collins, O. C., & Duffy, K. J. (2022). A mathematical model for the dynamics and control of malaria in Nigeria. In *Infectious disease modelling* (Vol. 7, pp. 728–741), 4.
Corrado, A., et al. (2006). *The new campaign finance sourcebook*. Brookings Institution Press.
Ezihe, E. K., et al. (2017). Seasonal distribution and micro-climatic factors influencing the abundance of the malaria vectors in south-east Nigeria. In *Journal of mosquito research* (Vol. 7).
Gabriel, O., Koske, J. K., Mutiso, J. M., et al. (2016). Transmission dynamics and optimal control of malaria in Kenya. In *Discrete Dynamics in Nature and society 2016*.
Gallup, J. L., & Sachs, J. D. (2000). The economic burden of malaria. In *CID working paper series*.
Griffin, J. T., et al. (2010). Reducing Plasmodium falciparum malaria transmission in africa: A model-based evaluation of intervention strategies. In *PLoS medicine* (Vol. 7), Article e1000324, 8.
Herdicho, F. F., Williams, C., Tasman, H., et al. (2021). An optimal control of malaria transmission model with mosquito seasonal factor. In *Results in physics* (Vol. 25), Article 104238.
Ippolito, M. M., et al. (2021). Antimalarial drug resistance and implications for the WHO global technical strategy. In *Current epidemiology reports* (Vol. 8, pp. 46–62).
Ma, B., Li, C., & Warner, J. (2019). Structured mathematical models to investigate the interactions between Plasmodium falciparum malaria parasites and host immune response. In *Mathematical biosciences* (Vol. 310, pp. 65–75).
Mandal, S., Sarkar, R. R., & Sinha, S. (2011). Mathematical models of malaria-a review. In *Malaria journal* (Vol. 10, pp. 1–19), 1.
Matuschewski, K. (2006). Getting infectious: Formation and maturation of Plasmodium sporozoites in the Anopheles vector. In *Cellular microbiology* (Vol. 8, pp. 1547–1556), 10.
Mueller, I., et al. (2022). Asia-pacific ICEMR: Understanding malaria transmission to accelerate malaria elimination in the asia pacific region. In *The American journal of tropical medicine and hygiene* (Vol. 107, p. 131), 4 Suppl.
Ndamuzi, E., & Gahungu, P. (2021). Mathematical modeling of Malaria transmission dynamics: Case of Burundi. In *Journal of applied mathematics and physics* (Vol. 9, pp. 2447–2460), 10.

Paton, D. G., et al. (2019). Exposing Anopheles mosquitoes to antimalarials blocks Plasmodium parasite transmission. In *Nature* (Vol. 567, pp. 239–243), 7747.
Prempeh, E. B. (2020). *Assessing the effects of indoor residual spraying (IRS) on malaria morbidity by anglogold malaria control programme in the amansie central district*. University of Cape Coast. PhD thesis.
Ren, Z., et al. (2016). Predicting malaria vector distribution under climate change scenarios in China: Challenges for malaria elimination. In *Scientific reports* (Vol. 6), Article 20604, 1.
Stresman, G. H. (2010). Beyond temperature and precipitation: Ecological risk factors that modify malaria transmission. In *Acta tropica* (Vol. 116, pp. 167–172), 3.
Traoré, B., Sangaré, B., Traoré, S., et al. (2017). A mathematical model of malaria transmission with structured vector population and seasonality. In *Journal of applied mathematics* (Vol. 2017).
Van den Driessche, P., & James, W. (2002). Reproduction numbers and sub-threshold endemic equilibria for compartmental models of disease transmission. In *Mathematical biosciences* (Vol. 180, pp. 29–48), 1-2.
Walker, P. G. T., et al. (2016). Estimating the most efficient allocation of interventions to achieve reductions in Plasmodium falciparum malaria burden and transmission in africa: A modelling study. In *The lancet global health* (Vol. 4, pp. e474–e484), 7.
World Bank. (2021). Incidence of malaria (per 1,000 population at risk) - Kenya. https://data.worldbank.org/indicator/SH.MLR.INCD.P3?end=2021&locations=KE&start=2000. (Accessed 12 September 2023).
World Health Organization. (2023). Malaria. https://www.who.int/news-room/fact-sheets/detail/malaria. (Accessed 15 September 2023).
World Health Organization, et al. (2020). In *The potential impact of health service disruptions on the burden of malaria: A modelling analysis for countries in sub-saharan africa*.
Xu, R., Zhang, S., & Zhang, F. (2016). Global dynamics of a delayed SEIS infectious disease model with logistic growth and saturation incidence. In *Mathematical methods in the applied sciences* (Vol. 39, pp. 3294–3308), 12.
Yaya, S., Uthman, O. A., Amouzou, A., & Bishwajit, G. (2018). Mass media exposure and its impact on malaria prevention behaviour among adult women in sub-saharan africa: Results from malaria indicator surveys. *Global health research and policy, 3*, 1–9.